Propagating coherent acoustic phonon wave packets in $In_xMn_{1-x}As/GaSb$

J. Wang, Y. Hashimoto,* and J. Kono†
Department of Electrical and Computer Engineering, Rice Quantum Institute, and Center for Nanoscale Science and Technology, Rice University, Houston, Texas 77005, USA

A. Oiwa‡
PRESTO, Japan Science and Technology Agency, 4-1-8 Honcho, Kawaguchi 332-0012, Japan

H. Munekata
Imaging Science and Engineering Laboratory, Tokyo Institute of Technology, 4259 Nagatsuta, Yokohama 226-8503, Japan

G. D. Sanders and C. J. Stanton
Department of Physics, University of Florida, Gainesville, Florida 32611, USA
(Received 10 May 2005; revised manuscript received 1 August 2005; published 25 October 2005)

We observe pronounced oscillations in the differential reflectivity of a ferromagnetic InMnAs/GaSb heterostructure using two-color pump-probe spectroscopy. Although originally thought to be associated with the ferromagnetism, our studies show that the oscillations instead result from changes in the position and frequency-dependent dielectric function due to the generation of coherent acoustic phonons in the ferromagnetic InMnAs layer and their subsequent propagation into the GaSb. Our theory accurately predicts the experimentally measured oscillation period and decay time as a function of probe wavelength.

DOI: 10.1103/PhysRevB.72.153311 PACS number(s): 75.50.Pp, 85.75.−d

Recently, there has been much interest in (III,Mn)V dilute magnetic semiconductors (DMS) with carrier-mediated ferromagnetism, a promising system for the realization of future semiconductor spintronic devices capable of performing information processing, data storage, and communication functions simultaneously.[1–3] InMnAs is the prototypical III-V DMS, being the first DMS to exhibit ferromagnetism and the first DMS in which cyclotron resonance was observed, evidence that at least some of the carriers are itinerant.[4–6]

Despite the fact that time-domain studies of the dynamic aspects of (III,Mn)Vs are more informative than static magnetization or electrical transport measurements, relatively few time-dependent studies have been attempted. In this Brief Report, we report on our time-dependent femtosecond transient reflectivity measurements on an InMnAs/GaSb heterostructure using two-color pump-probe spectroscopy. In addition to changes in the reflectivity associated with ultrashort carrier lifetimes (~2 ps) and multilevel carrier decay dynamics which we attribute to a large density of bound states and a high concentration of Mn *p*-type dopants, we observe pronounced oscillations in the differential reflectivity signal. While originally the oscillations were believed to originate from the ferromagnetism (since they were not observed in similiar systems without Mn doping), a systematic study shows that they instead result from the generation of coherent phonons in the InMnAs layer which then propagate into the GaSb. The period and the characteristic decay time of the transient reflectivity oscillations are consistent with a propagating coherent acoustic phonon wave-packet model.[7]

While femtosecond spectroscopy has previously been used for generating and detecting coherent phonons in many materials [e.g., optical phonons in bulk semiconductors, metals (Bi, Sb), and superconductors; acoustic phonons in InGaN/GaN-based semiconductor heterostructures[7–13]], only recently has there been interest in the application of this technique to probing coherent excitations (e.g., phonons and magnons) in strongly correlated electronic systems.[14,15] These innovative studies further demonstrate the potential of transient reflectivity spectroscopy to unravel the subtle interplay between lattice and spin excitations.

The main Mn-doped sample studied was a *p*-InMnAs/GaSb heterostructure grown by low-tempeature molecular beam epitaxy (LTMBE). The sample [shown schematically in Fig. 1(a)] consisted of a 25-nm *p*-type InMnAs layer and an 820-nm GaSb buffer layer grown on top of a (100) GaAs substrate. The hole density and mobility in the InMnAs layer, as estimated by Hall measurements, were 1.1×10^{19} cm^{-3} and 323 cm^2/V s, respectively. Detailed growth conditions and sample information can be found in Ref. 16.

In order to separate various nonlinear effects and extract information on the dynamical response of the InMnAs/GaSb heterostructure, we used a two-color, selective pumping scheme[17] shown schematically in Fig. 1(a). A 140 fs, midinfrared (MIR) 2 μm pump beam from an optical parametric amplifier (OPA) was used to create carriers in InMnAs with an excess kinetic energy of ~0.2 eV. Pumping at this photon energy allowed us to selectively photoexcite carriers in the InMnAs layer but not in the GaSb buffer layer or GaAs substrate. A white-light continuum probe beam (500–1400 nm, ~340 fs), generated by focusing a small fraction of the intense 775 nm beam from a chirped pulse amplifier (Model CPA-2010, Clark-MXR, Inc.) onto a sapphire crystal, allowed us to probe energies far above the quasi-Fermi level of the optically excited carriers.

Typical time-dependent differential reflectivity data are shown in Fig. 1(b). After photoexcitation, the reflectivity shows a sharp drop followed by a rapid rise and sign change

 ©2005 The American Physical Society

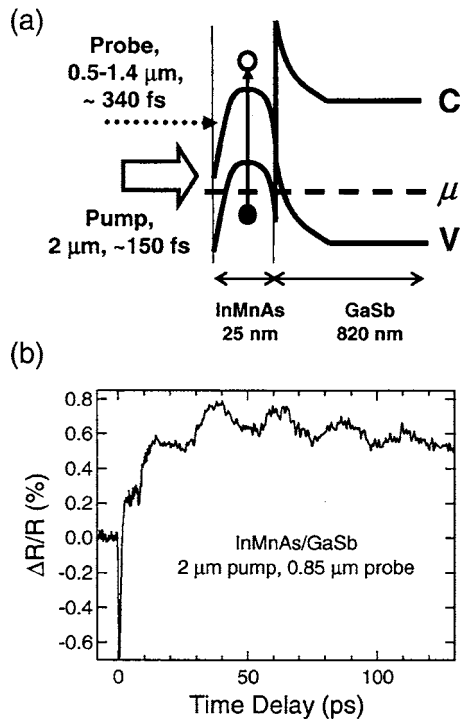

FIG. 1. (a) Schematic diagram of two-color pump-probe differential reflectivity experiment in an InMnAs/GaSb heterostructure. The pump photoexcites carriers only in the InMnAs layer and the transient differential reflectivity is probed at higher energies. (b) Typical time-resolved differential reflectivity data, showing an initial drop followed by oscillations in reflectivity.

in a time less than ~2 ps. At longer times (several hundred ps) periodic oscillations are observed with a period of ~23 ps superimposed on a very slow decay. The initial sharp drop in reflectivity is believed to result from free carrier Drude absorption by the hot photogenerated carriers. The carriers relax back to quasiequilibrium distributions through the emission of confined LO phonons and the ultrafast trapping of electrons (by As_{Ga} antisite defects) and holes (by Ga vacancies) by the midgap states introduced by LTMBE growth. This alters the dielectric function of the heterostructure through changes in the electron and hole distribution functions and gives rise to the sharp increase and sign change in the differential reflectivity seen in Fig. 1(b). Over much longer times, the quasiequilibrium electrons and holes recombine across the gap causing the differential reflectivity to return to zero. The beginning of this slow decay can be seen in Fig. 1(b).

Initially, the oscillations were thought to originate from the Mn ions and possibly the ferromagnetism since they were not observed in similar samples without Mn. However, an applied external magnetic field of 0, 5, and 9.5 T did not change the oscillation period as shown in Fig. 2(a). This rules out magnons or quantum beats between Landau levels as a source of the oscillations. Furthermore, our field-dependent experiments show that magnetism does not play a role in the observed oscillations.

Next, we varied the pump fluence as shown in Fig. 2(b). For pump fluences of 0.7, 3.5, and 10 mJ/cm^2, the intensity of the oscillation changed but the frequency did not. Varying

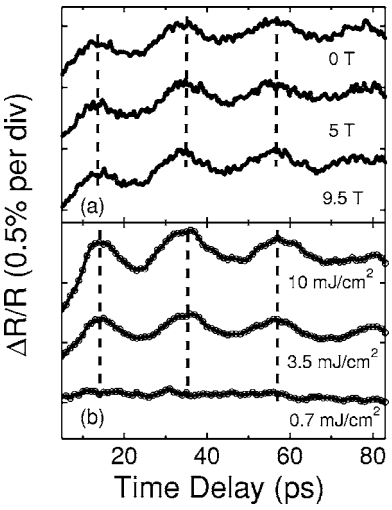

FIG. 2. Two-color pump-probe differential reflectivity oscillations in an InMnAs/GaSb heterostructure. The dependence of the oscillations on magnetic field is shown in (a) while the dependence on pump power is shown in (b). The oscillation period does not change as shown by the vertical dashed lines.

the pump fluence increases the photoexcited carrier density. Since the plasma frequency increases with the total carrier concentration, we would expect the oscillation period to increase with increasing pump fluence if it were related to plasmons. Since the oscillation period is independent of pump fluence, we rule out plasmons as the cause of the oscillations.

A final possibility is that coherent phonons could be excited in the InMnAs epilayer, since they have previously been observed in InGaN/GaN epilayers,[7,11] though InGaN/GaN has a wurtzite structure and as a result, strain can lead to large built-in piezoelectric fields (unlike InMnAs, which has a zinc-blende structure). The theory for the generation and propagation of coherent acoustic phonons in InGaN/GaN nanostructures having the wurzite structure has been described in Ref. 18 (see the erratum in Ref. 19). Reference 20 provides a good review of both experimental and theoretical aspects of coherent acoustic phonon generation in piezoelectric nitride-based semiconductor heterostructures. Generation of coherent acoustic phonons comes about from the electron-phonon interaction.[21–23] In nitride-based heterostructures such as GaN/InGaN large amplitude coherent acoustic phonon wave packets can be generated through the piezoelectric and deformation potential electron-phonon interactions with the piezoelectric interaction being dominant.

In contrast to the nitrides, the InMnAs/GaSb heterostructure has a zinc-blende structure. Consequently, coherent acoustic phonons cannot be generated (for [100]-grown samples) through the *piezoelectric* electron-phonon interaction. They can, however, be generated through the *deformation potential* electron-phonon interaction, but their amplitudes are weak. However, we can detect the coherent phonon oscillations in the differential reflectivity through a fortuitous circumstance. The wavelength-dependent GaSb dielectric function is very sensitive to small changes in strain in the vicinity of the E_1 (L-valley) transition centered at approxi-

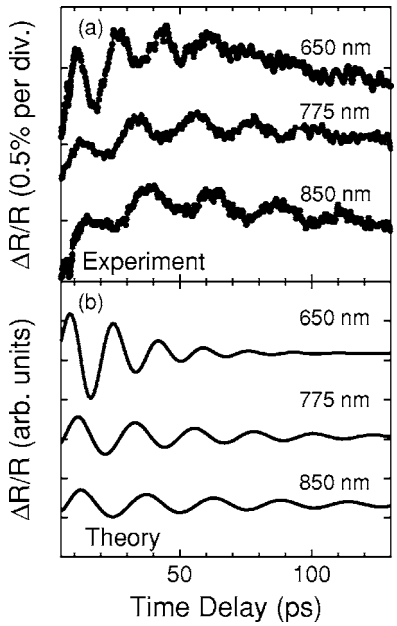

FIG. 3. Experimental (a) and theoretical (b) coherent phonon differential reflectivity oscillations for probe wavelengths of 650, 775, and 850 nm.

mately 600 nm, which is close to our probe region.

We developed a theoretical model for the transient differential reflectivity in our InMnAs/GaSb structure based on a Boltzmann equation formalism. The photoexcited carriers in the ferromagnetic quantum well are assumed to be completely confined and electronic states near the band edge are treated in an eight-band effective mass model including conduction electrons, heavy holes, light holes, and split-off holes. The experiments were carried out in a ferromagnetic heterostructure where Mn impurity spins influence the band structure, so the effect of Mn impurity spins on the itinerant carriers is also included. Photogeneration of carriers in the quantum well is treated using Fermi's golden rule and carrier scattering by confined LO phonons in the quantum well is accounted for. From the time-dependent carrier densities, the generation and propagation of coherent acoustic phonons in zinc-blende materials due to deformation potential electron-phonon interaction can be modeled by solving a loaded string equation for the propagating coherent phonon lattice displacement. This is described in Ref. 18 for wurzite materials and contains a piezoelectric electron-phonon term which vanishes in the zinc-blende case. Changes in the position- and frequency-dependent dielectric function due to coherent acoustic phonons are computed, and the time-dependent reflectivity at the probe wavelength is obtained by globally solving Maxwell's equations in the entire structure.

In Fig. 3 the coherent phonon differential reflectivity oscillations are shown as a function of time delay for probe wavelengths of 650, 775, and 850 nm. The theoretical curves in Fig. 3(b) agree well with the experimentally measured differential reflectivity in Fig. 3(a) after subtraction of the transient background signal. As the probe wavelength approaches the GaSb E_1 transition near 600 nm, the amplitude of the differential reflectivity oscillations increase due to the enhanced sensitivity of the GaSb dielectric function to the strain pulse.

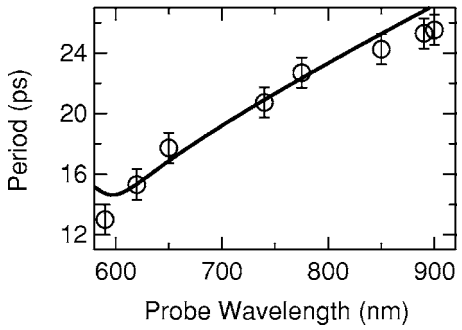

FIG. 4. Experimental coherent phonon differential reflectivity oscillation period vs probe wavelength (open circles). The solid line shows the theoretical estimates.

The damping of the differential reflectivity oscillations seen in Fig. 3 is due to the finite penetration length of our probe inside the GaSb layer. The periodic oscillations in the differential reflectivity can be modeled by

$$\frac{\Delta R}{R}(t) \sim \alpha \cos\left(\frac{4\pi C_s n}{\lambda} t - \Phi\right) e^{-t/\mathcal{T}}, \tag{1}$$

where Φ and $\mathcal{T}$ are the phase and decay time, $\lambda = 2\pi c/\omega$ is the probe wavelength, C_s is the acoustic sound speed, and n is the refractive index at the probe wavelength. From fits to the data, the decay time for a probe wavelength of 650 nm is found to be $\sim$45 ps. The decay time is approximately $\mathcal{T} = \lambda/(4\pi\, C_s\, k)$, where k is the extinction coefficient at the probe wavelength. A numerical estimate yields a value of 41 ps for the decay time in reasonable agreement with experiment seen in Fig. 3.

The differential reflectivity oscillation period increases with wavelength from 650 to 850 nm. The period of the reflectivity oscillations can be easily understood. The propagating strain pulse gives rise to a perturbation in the GaSb dielectric function, which propagates at the acoustic sound speed. The sample thus acts as a Fabry-Perot interferometer, and a simple geometrical optics argument shows that the period for the reflectivity oscillations due to the propagating coherent acoustic phonon wave packet is approximately[11] $T = \lambda/[2C_s n(\lambda)]$ where $C_s = 3.97 \times 10^5$ cm/s is the longitudinal acoustic (LA) sound speed in the GaSb barrier and $n(\lambda)$ is the wavelength dependent refractive index. At the wavelength of the probe (850 nm), $n(\lambda) \approx 4.24$ and we calculate the period of the differential reflectivity oscillations to be $T = 25.2$ ps, which is in close agreement with the observed oscillation period of 24 ps seen in Fig. 1(b). In Fig. 4 we have plotted the experimentally measured coherent phonon differential reflectivity oscillation periods as a function of probe wavelength as open circles. The solid line shows the oscillation period vs probe wavelength estimated using the simple geometrical optics argument and taking the wavelength dependence of the refractive index in GaSb into account. The excellent agreement between theory and experiment clearly demonstrates that the reflectivity oscillations are the result of propagating coherent acoustic phonons in the GaSb barrier.

The period of the reflectivity oscillation is due to Fabry-Perot interference. Taking account of surface reflection at the

InMnAs/air interface, the temporal width τ of the pulse is obtained by dividing twice the well width by the LA sound speed. Thus $\tau \sim 12.6$ ps.

In summary, we have performed time-dependent two-color differential reflectivity measurements on a ferromagnetic InMnAs/GaSb heterostructure. In addition to observing changes in the reflectivity due to ultrashort carrier dynamics, we have observed reflectivity oscillations resulting from coherent phonon generation in the InMnAs layer. The propagation of these coherent, localized "strain pulses" into and through the GaSb buffer layer results in a position and frequency-dependent dielectric function. Our theoretical calculations accurately reproduce the experimental results. These results offer the intriguing possibility of future devices using coherent phonons to interact with the Mn spins in much the same manner that photoexcited carriers have been used to manipulate ferromagnetism.

We thank Xiangfeng Wang for technical help. This work was supported by NSF (through DMR-0134058, DMR-0325474, and INT-0221704), DARPA (through MDA972-00-1-0034), and ONR (through N000140410657).

*Present address: Graduate School of Science and Technology, Chiba University, Chiba, Japan.
†Corresponding author. Electronic address: kono@rice.edu
‡Present address: Department of Applied Physics, University of Tokyo, 7-3-1 Hongo, Bunkyo-ku, Tokyo 113-8656, Japan.

[1] I. Žutić, J. Fabian, and S. Das Sarma, Rev. Mod. Phys. **76**, 323 (2004).
[2] H. Ohno, Science **281**, 951 (1998).
[3] S. A. Wolf, D. D. Awschalom, R. A. Buhrman, J. M. Daughton, S. von Molnár, M. L. Roukes, A. Y. Chtchelkanova, and D. M. Treger, Science **294**, 1488 (2001).
[4] M. A. Zudov, J. Kono, Y. H. Matsuda, T. Ikaida, N. Miura, H. Munekata, G. D. Sanders, Y. Sun, and C. J. Stanton, Phys. Rev. B **66**, 161307(R) (2002).
[5] G. D. Sanders, Y. Sun, F. V. Kyrychenko, C. J. Stanton, G. A. Khodaparast, M. A. Zudov, J. Kono, Y. H. Matsuda, N. Miura, and H. Munekata, Phys. Rev. B **68**, 165205 (2003).
[6] Y. H. Matsuda, G. A. Khodaparast, M. A. Zudov, J. Kono, Y. Sun, F. V. Kyrychenko, G. D. Sanders, C. J. Stanton, N. Miura, S. Ikeda, Y. Hashimoto, S. Katsumoto, and H. Munekata, Phys. Rev. B **70**, 195211 (2004).
[7] R. Liu, C. S. Kim, G. D. Sanders, C. J. Stanton, J. S. Yahng, Y. D. Jho, K. J. Yee, E. Oh, and D. S. Kim, cond-mat/0310654, Phys. Rev. B (to be published).
[8] G. C. Cho, W. Kütt, and H. Kurz, Phys. Rev. Lett. **65**, 764 (1990).
[9] A. Bartels, T. Dekorsy, H. Kurz, and K. Köhler, Phys. Rev. Lett. **82**, 1044 (1999).
[10] C. K. Sun, J. C. Liang, and X. Y. Yu, Phys. Rev. Lett. **84**, 179 (2000).
[11] J. S. Yahng, Y. D. Jho, K. J. Yee, E. Oh, J. C. Woo, D. S. Kim, G. D. Sanders, and C. J. Stanton, Appl. Phys. Lett. **80**, 4723 (2002).
[12] T. K. Cheng, J. Vidal, H. Zeigler, G. Dresselhaus, and E. P. Ippen, Appl. Phys. Lett. **59**, 1923 (1991).
[13] J. M. Chwalek, C. Uher, J. F. Whitaker, G. A. Mourou, and J. A. Agostinelli, Appl. Phys. Lett. **58**, 980 (1991).
[14] D. Lim, R. D. Averitt, J. Demsar, A. J. Taylor, N. Hur, and S. W. Cheong, Appl. Phys. Lett. **83**, 4800 (2003).
[15] R. Arita, Y. Suwa, K. Kuroki, and H. Aoki, Phys. Rev. Lett. **88**, 127202 (2002).
[16] T. Slupinski, A. Oiwa, S. Yanagi, and H. Munekata, J. Cryst. Growth **237–239**, 1326 (2002).
[17] J. Wang, G. A. Khodaparast, J. Kono, T. Slupinski, A. Oiwa, and H. Munekata, J. Supercond. **16**, 373 (2003).
[18] G. D. Sanders, C. J. Stanton, and C. S. Kim, Phys. Rev. B **64**, 235316 (2001).
[19] G. D. Sanders, C. J. Stanton, and C. S. Kim, Phys. Rev. B **66**, 079903(E) (2002).
[20] G.-W. Chern, C.-K. Sun, G. D. Sanders, and C. J. Stanton, in *Topics in Applied Physics*, edited by K.-T. Tsen (Springer-Verlag, New York, 2004), Vol. 92, pp. 339–394.
[21] A. V. Kuznetsov and C. J. Stanton, Phys. Rev. Lett. **73**, 3243 (1994).
[22] A. V. Kuznetsov and C. J. Stanton, Phys. Rev. B **51**, 7555 (1995).
[23] A. V. Kuznetsov and C. J. Stanton, in *Ultrafast Phenomena in Semiconductors*, edited by F. Tsen (Springer-Verlag, New York, 2001), pp. 353–403.